



HAL
open science

Characterization of nonlinear, nonstationary systems in operational modal analysis using wavelet transform

Raphaël Carpine, Pierre Argoul, Claude Rospars

► To cite this version:

Raphaël Carpine, Pierre Argoul, Claude Rospars. Characterization of nonlinear, nonstationary systems in operational modal analysis using wavelet transform. ISMA-USD Noise and Vibration Engineering Conference 2022, Sep 2022, Louvain, Belgium. hal-03779116

HAL Id: hal-03779116

<https://hal.science/hal-03779116v1>

Submitted on 16 Sep 2022

HAL is a multi-disciplinary open access archive for the deposit and dissemination of scientific research documents, whether they are published or not. The documents may come from teaching and research institutions in France or abroad, or from public or private research centers.

L'archive ouverte pluridisciplinaire **HAL**, est destinée au dépôt et à la diffusion de documents scientifiques de niveau recherche, publiés ou non, émanant des établissements d'enseignement et de recherche français ou étrangers, des laboratoires publics ou privés.

Characterization of nonlinear, nonstationary systems in operational modal analysis using wavelet transform

R. Carpine, P. Argoul, C. Rospars

Univ Gustave Eiffel, MAST-EMGCU,

F-77454 Marne-la-Vallée, France

e-mail: raphael.carpine@univ-eiffel.fr

Abstract

This study focuses on the characterization of nonstationary, weakly nonlinear, weakly damped mechanical systems, subjected to an unknown ambient excitation modeled as white Gaussian noise. A theoretical analysis using a novel approach of a one degree of freedom system, whose dynamic response is investigated in time domain as a Markov process, allows simple relations to be established on the expectation and standard deviation of its amplitude and instantaneous frequency. This theoretical study of the system behavior is coupled with the use of the Continuous Wavelet Transform (CWT) ridge, which gives the amplitude and instantaneous frequency of its vibrations. A discussion on the tuning of the mother wavelet function for the analysis of these signals is presented. A simple procedure based on the use of the CWT, characterizing the system's nonlinear, nonstationary behavior, is then proposed. Finally, numerical simulations are carried out, and the proposed method is implemented. Results show good agreement with those of the theoretical study.

1 Introduction

Structural Health Monitoring (SHM) techniques capable of accurately monitoring the structural response to load conditions in real time, detecting damage in the structure, and reporting the location and nature of that damage are developing currently very rapidly in the world of civil engineering infrastructure. Detecting and characterizing nonlinearities in the dynamical behavior of systems and structures has become an important issue in the field of SHM, because it can be linked in some cases to damage [1, 2]. However, as SHM is generally based on output-only signals where ambient excitation is uncontrolled and unknown, this detection constitutes a challenge. In this paper, we propose a new method to characterize nonlinear, nonstationary systems under unknown white Gaussian noise. It is based on the wavelet transform, because of its abilities in time-frequency signal analysis and instantaneous frequency estimation.

Developed by French researchers in the early 1980s, the wavelet transform has since made significant progress, especially in the fields of signal processing and image processing [3]. Its field of application also extends to the treatment of vibratory responses of mechanical structures or engineering structures, in particular through the use of the Continuous Wavelet Transform (CWT), of which the books [4, 5] present an excellent overview. CWT is a time-frequency analysis tool, particularly adapted to signals resulting from modal analysis. Indeed, its ability to separate the amplitudes $A_k(t)$ and phases $\Phi_k(t)$ of the different components $A_k(t) \cos \Phi_k(t)$ of a signal allows, in the case of transient vibratory responses of mechanical systems, to easily identify their modal parameters. We can for example mention the case of free responses of linear systems, often analyzed from the ridges of their CWT, and of which one can find a presentation in [6], with a discussion on the tuning of the time-frequency resolution of the wavelet transform using its quality factor, or in [7], which deals with free responses of linear systems with non-proportional damping. For free responses of nonlinear systems, the use of the Krylov-Bogoliubov method [8] is often coupled with that of wavelet analysis for an estimation of modal and nonlinear parameters [9, 10]. Finally, in the case of linear systems under ambient excitation, the use of CWT usually requires an additional filtering (or transformation) step. This filtering can be done a posteriori, with for example the use of the singular value decomposition [11], or

a priori, by transforming this ambient response into a free response, from the autocorrelation and crosscorrelation of the signals [12, 13], or from the random decrement technique [14].

However, these filtering techniques are not suitable for nonlinear systems under ambient excitation, because they are based on the use of the convolution product between the impulse response of the system and excitation, which is relevant only in the linear case. This study therefore proposes a new technique, based on the CWT, to characterize nonlinear, nonstationary systems under ambient excitation. We will limit ourselves to mechanical systems with low nonlinear stiffness, low linear damping (classical assumption in structural dynamics), and by simplification, with one degree of freedom. The ambient excitation will be modeled by a white Gaussian noise.

The paper is divided into three parts. The first part is devoted to an analytical study of linear and nonlinear systems under ambient excitation, allowing the characterization of their dynamic behavior from a time-frequency point of view, suitable for the subsequent use of wavelet analysis. Then, the identification method based on CWT is presented, with some preliminary reminders, and the wavelet parameters settings are detailed. Finally, two simple case studies based on numerical simulations allow to test the implementation of the proposed method, and to assess the accuracy of the theoretical results.

2 Theoretical analysis

2.1 Linear, stationary oscillator

We consider in all this study an oscillator with mass m , stiffness k and damping coefficient c , linear and stationary at first, weakly damped and subjected to an excitation w . Its equation of motion is written in its normalized form:

$$\ddot{x} + 2\zeta\omega_n\dot{x} + \omega_n^2x = \frac{w}{m}, \quad (1)$$

with x its displacement, $\omega_n = (k/m)^{1/2}$ its natural angular frequency, $\zeta = c/2(km)^{1/2}$ its damping ratio, $\omega_d = \omega_n(1 - \zeta^2)^{1/2}$ its damped angular frequency, $\mu = \zeta\omega_n$ its damping constant and $\lambda = i\omega_d - \mu$ its pole. Its free response x_{free} , when $w = 0$, can be expressed as:

$$x_{\text{free}}(t) = A_0e^{-\mu t} \cos(\omega_d t + \varphi_0), \quad (2)$$

where A_0 and φ_0 are constants that depend on the initial conditions.

2.1.1 Discretization of the input and response signals

For simplification purposes, continuous input w is replaced by a discrete form \tilde{w} , defined as:

$$\tilde{w}(t) = \sum_{n=-\infty}^{+\infty} w_n \delta(t - t_n), \quad (3)$$

where $t_n = n\Delta t$, w_n is defined as the integral of w from $t_n - \Delta t/2$ to $t_n + \Delta t/2$, and δ is the Dirac function. Then, we assume that excitation is a white Gaussian noise, which implies that (w_n) is a sequence of independent and identically distributed random variables, following a normal distribution:

$$\forall n, w_n \sim \mathcal{N}(0, \sigma^2). \quad (4)$$

Next, displacement x is discretized as well. Using Eqs. (2) and (3), we get $x(t_n + \tau) = A_n \cos(\omega_d \tau + \varphi_n) e^{-\mu \tau}$ for $\tau \in (0, \Delta t)$, which leads us to introduce the complex, discrete position $\underline{X}_n = A_n e^{i\varphi_n}$. The following recurrence relation is then derived from Eqs. (1) et (3):

$$\underline{X}_{n+1} = \underline{X}_n e^{\lambda \Delta t} - i \frac{w_{n+1}}{m\omega_d}. \quad (5)$$

Next, introducing $P = 2\pi/(\omega_d\Delta t)$ the number of time increment in a period of the damped system, and by assuming that $P \in \mathbb{N}$ (Δt can be adjusted to that purpose), we get from Eq. (5) a new recurrence relation:

$$\underline{X}_{n+P} = r_0\underline{X}_n - \frac{i}{m\omega_d} \sum_{j=1}^P w_{n+j} e^{\lambda(P-j)\Delta t}, \quad (6)$$

with $r_0 = e^{-2\pi\mu/\omega_d} < 1$. Because the system is assumed to be weakly damped, i.e. $\zeta \ll 1$, its pole λ can be approximated by its imaginary part $\lambda \approx i\omega_d$, and we introduce a new random variable $\underline{W}_{P,n}$, defined as:

$$\underline{W}_{P,n} = \sum_{j=1}^P w_{n+j} e^{i\omega_d(P-j)\Delta t} \approx \sum_{j=1}^P w_{n+j} e^{\lambda(P-j)\Delta t}. \quad (7)$$

It can be shown from the definition of w_k given in Eq. (4) that random variables $\text{Re}\{\underline{W}_{P,n}\}$ and $\text{Im}\{\underline{W}_{P,n}\}$ are uncorrelated and both follow a centered normal distribution of variance $\pi\sigma^2/(\omega_d\Delta t)$.

We now focus on the system evolution on one period, from a known state, i.e. $\underline{X}_{n+P}|\underline{X}_n$. For that purpose, we introduce the random variable $\underline{Y}_{P,n}$ defined as:

$$\underline{Y}_{P,n} = r_0\underline{X}_n - \frac{i}{m\omega_d} \underline{W}_{P,n} \approx \underline{X}_{n+P}, \quad (8)$$

where the approximation is insured by Eq. (7). Random variables $\text{Re}\{\underline{Y}_{P,n}\}|\underline{X}_n$ and $\text{Im}\{\underline{Y}_{P,n}\}|\underline{X}_n$ follow uncorrelated normal distributions, with expectations $r_0\text{Re}\{\underline{X}_n\}$ and $r_0\text{Im}\{\underline{X}_n\}$ respectively, and both with variance $\pi\sigma^2/(m^2\omega_d^3\Delta t)$. A graphical representation of the probability density of $\underline{Y}_{P,n}|\underline{X}_n$ in the complex plane is given in Fig. 1.

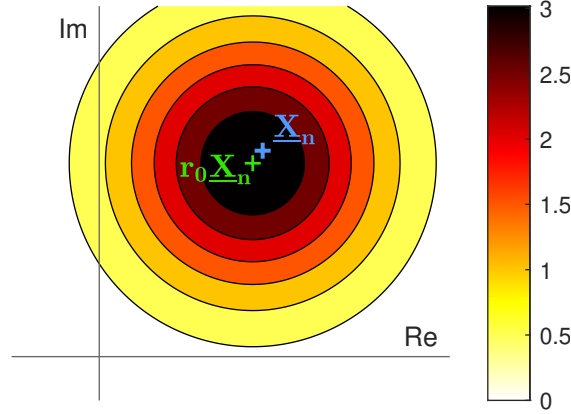


Figure 1: Representation of the probability density of $\underline{Y}_{P,n}|\underline{X}_n$ in the complex plane (the green cross is at the center of the probability density).

2.1.2 Amplitude analysis

The variation of amplitude over a period is given by the study of $|\underline{Y}_{P,n}|\underline{X}_n$, whose expectation can be expressed as:

$$\mathbb{E} [|\underline{Y}_{P,n}|\underline{X}_n] \approx r_0|\underline{X}_n| + \frac{\pi\sigma^2}{2r_0m^2\omega_d^3\Delta t|\underline{X}_n|}. \quad (9)$$

This way, for a high value of $|\underline{X}_n|$, the amplitude of oscillation is expected to decrease, and on the contrary for a low value of $|\underline{X}_n|$, it is expected to increase. The limit case for which the amplitude is expected to be

sustained is reached for an amplitude that we will call A_{ref} , which by Eq. (9) equals:

$$A_{\text{ref}} \approx \frac{\sigma}{2m\omega_d\sqrt{r_0}\mu\Delta t}. \quad (10)$$

To estimate the derivative of the amplitude of oscillation when it is equal to its reference value A_{ref} , we are now considering the variance of $|\underline{Y}_{P,n}| \mid \underline{X}_n$, which can be written as:

$$\text{Var} [|\underline{Y}_{P,n}| \mid \underline{X}_n] \approx \frac{\pi\sigma^2}{m^2\omega_d^3\Delta t}. \quad (11)$$

We then obtain an estimate of this derivative, which we will call \dot{A}_{ref} :

$$\dot{A}_{\text{ref}} = \frac{1}{P\Delta t} \sqrt{\text{Var} (|\underline{Y}_{P,n}| \mid |\underline{X}_n| = A_{\text{ref}})} \approx \frac{\sigma}{2m\sqrt{\pi\omega_d\Delta t}}. \quad (12)$$

Finally, from Eqs. (10) and (12) and the hypothesis of low damping, we get:

$$\frac{\dot{A}_{\text{ref}}}{A_{\text{ref}}} \ll \omega_d. \quad (13)$$

Therefore, we can consider that over a period of oscillation of the system, its amplitude remains approximately constant.

2.1.3 Phase analysis

We now define $\Omega_{P,n}$, the instantaneous angular frequency of the system over one period, as:

$$\Omega_{P,n} = \frac{1}{P\Delta t} \left(2\pi + \arg \left(\frac{\underline{X}_{n+P}}{\underline{X}_n} \right) \right) \approx \omega_d \left(1 + \frac{1}{2\pi} \arg \left(\frac{\underline{Y}_{P,n}}{\underline{X}_n} \right) \right). \quad (14)$$

Its expectancy can then be computed from Eq. (8):

$$\mathbb{E} [\Omega_{P,n} \mid \underline{X}_n] \approx \omega_d, \quad (15)$$

along with its variance:

$$\text{Var} (\Omega_{P,n} \mid \underline{X}_n) \approx \left(\frac{\sigma}{2m|\underline{X}_n|\sqrt{\pi\omega_d\Delta t}} \right)^2. \quad (16)$$

Thus, as shown in Eq. (15), the instantaneous angular frequency of the system under ambient excitation is on average equal to that of its free response, ω_d . However, this instantaneous angular frequency shows a certain dispersion around its mean, whose standard deviation is inversely proportional to the oscillation amplitude of the system (see Eq. (16)). This dispersion can be explained by the fact that for small amplitudes, the excitation force w to which the system is subjected is no longer negligible in front of the inertia $m\ddot{x}$ and stiffness kx forces, which govern its free response behavior.

2.2 Nonlinear, stationary oscillator

We now consider that the system has a weak stiffness nonlinearity, modeled by an additional restoring force $g(x)$. Eq. (1) thus becomes:

$$\ddot{x} + 2\zeta\omega_n\dot{x} + \omega_n^2x + \frac{g(x)}{m} = \frac{w}{m}, \quad (17)$$

where $|g(x)| \ll |m\omega_n^2x|$.

2.2.1 Free response

In the case of a free response x_{free} of the system, i.e. for a null excitation $w = 0$, one can use the first-order Krylov-Bogoliubov approximation [8], which results in:

$$x_{\text{free}}(t) \approx A_{\text{free}}(t) \cos(\omega_n t + \varphi_{\text{free}}(t)), \quad (18)$$

where A_{free} and φ_{free} vary slowly with respect to the period of the system, and verify the following system of differential equations:

$$\begin{bmatrix} \dot{A}_{\text{free}} \\ \dot{\varphi}_{\text{free}} \end{bmatrix} = \begin{bmatrix} H_A(A_{\text{free}}) \\ H_\varphi(A_{\text{free}}) \end{bmatrix}, \quad (19)$$

where H_A and H_φ are functions depending only on A_{free} , which will not be detailed here. Thus, for a given amplitude A_0 , the nonlinear system exhibits a behavior similar to that of a linear system whose pole $\tilde{\lambda}(A_0)$ can be written:

$$\tilde{\lambda}(A_0) = i(\omega_n + H_\varphi(A_0)) + \frac{H_A(A_0)}{A_0}. \quad (20)$$

For the real part of pole $\tilde{\lambda}(A_0)$, the Krylov-Bogoliubov method gives, as for the linear case, $H_A(A_0)/A_0 = -\mu$. For its imaginary part, we will use $\tilde{\omega}(A_0)$, the angular frequency of the nonlinear undamped system at amplitude A_0 (i.e. its response to Eq. (17) by replacing ζ and w by 0) rather than $\omega_n + H_\varphi(A_0)$, because numerical simulations show that it is a better approximation for weakly damped systems in free response. This higher precision is due to the relatively low influence of damping on free response frequency, as evidenced by the linear case where it is of the second order on ζ , which is typically very low in mechanical systems. The pole can thus be written:

$$\tilde{\lambda}(A_0) = i\tilde{\omega}(A_0) - \mu. \quad (21)$$

2.2.2 Ambient response

Finally, to deal with the case where the system is subjected to an ambient excitation, characterized by Eqs. (3) and (4), we first notice that the amplitude of the oscillations varies slowly with respect to their period (Eq. (13)), and that it can therefore be considered constant over one period. As explained previously, we then have an analogous behavior to that of a linear system, whose pole is characterized by Eq. (21). Thus all the results stated for the linear system apply, in particular Eq. (15) which becomes:

$$\mathbb{E} [\Omega_{P,n} | \underline{X}_n] \approx \tilde{\omega}(|\underline{X}_n|). \quad (22)$$

The expectancy of the instantaneous angular frequency of the nonlinear system under ambient excitation is therefore approximately equal to that of its free response.

2.3 Nonlinear, nonstationary oscillator

It is now assumed, in addition to the nonlinearity, that the parameters of the system, m , ω_n , ζ and g , are time dependent. This dependency is supposed to be slow compared to the period of the system, i.e. $|\dot{m}(t)/m(t)| \ll \omega_n(t)$ for mass m , and so on.

Similarly to the nonlinear, stationary system, we notice that over one period, the parameters of the system can be considered constant, and its behavior is therefore analogous to that of a linear system. Eq. (22) thus becomes:

$$\mathbb{E} [\Omega_{P,n} | \underline{X}_n] \approx \tilde{\omega}(t_n, |\underline{X}_n|), \quad (23)$$

where $\tilde{\omega}(t, A)$ denotes the angular frequency of the undamped nonlinear nonstationary system at time t and amplitude A .

Additionally, one particular case that deserves consideration here is when the system parameters can be written as functions of one or an array of known explanatory variables, denoted κ . In this case, Eq. (23)

becomes:

$$\mathbb{E} [\Omega_{P,n} | \underline{X}_n] \approx \tilde{\omega}(\kappa_n, |\underline{X}_n|), \quad (24)$$

where $\kappa_n = \kappa(t_n)$. For mechanical systems, these variables can be environmental factors such as temperature or humidity, or quasistatic loads for instance. In the latter case, the nonstationarity results from the shift of the equilibrium position that effectively changes the nonlinearity. Indeed, by replacing w by $F + w$ in Eq. (17), where F is a slowly varying additive force, it can be rewritten as:

$$\ddot{x}_{\text{dyn}} + 2\zeta\omega_n\dot{x}_{\text{dyn}} + \omega_n^2x_{\text{dyn}} + \frac{g(x_{\text{stat}} + x_{\text{dyn}}) - g(x_{\text{stat}})}{m} = \frac{w}{m}, \quad (25)$$

where x_{stat} is the quasistationary response of the system to F that satisfies $m\omega_n^2x_{\text{stat}} + g(x_{\text{stat}}) = F$ and whose time derivatives are neglected due to its slow variations, and x_{dyn} is the ‘‘dynamic’’ response of the system defined as $x_{\text{dyn}} = x - x_{\text{stat}}$. Eq. (25) is therefore a special case of nonlinear, nonstationary system, where the explanatory variable is x_{stat} .

3 Use of the Continuous Wavelet Transform

3.1 Definition and general properties

The Continuous Wavelet Transform (CWT) is a time-frequency analysis tool, particularly suited to the study of modulated oscillatory signals [4, 6]. We propose the following definition, for a signal u :

$$\mathbb{T}_\psi[u](t, f) = 2\pi f \int_{-\infty}^{+\infty} u(\tau)\psi(2\pi f(t - \tau)) \, d\tau, \quad (26)$$

where ψ denotes a complex function called the mother wavelet. This definition written directly in the time-frequency plane, instead of the classical definition in the time-scale plane, allows an easier use of the tool. However, it requires a normalization and a centering of the mother wavelet in the Fourier domain, which we will take for granted in the following. We will use the Morlet’s complex wavelet ψ_Q , for its good mathematical properties (in particular its minimal uncertainty in the time-frequency plane $\mu_\psi = 1/2$), making it particularly adapted to the analysis of amplitude and phase modulated signals. It is expressed as:

$$\psi_Q(\theta) = \frac{1}{Q\sqrt{\pi}} \exp(i\theta) \exp\left(-\frac{\theta^2}{4Q^2}\right), \quad (27)$$

where Q is a parameter of the mother wavelet called quality factor, characterizing its dispersion in the Fourier domain [6, 7]. As previously mentioned, ψ_Q is normalized and centered in the Fourier domain.

For a modulated oscillatory signal u such as:

$$u(t) = A(t) \cos \varphi(t), \quad (28)$$

with slow variations of A with respect to $\dot{\varphi}$, we obtain the following relations [4] on the ridge of the transform f_r , defined as:

$$f_r(t) = \underset{f}{\operatorname{argmax}} |\mathbb{T}_\psi[u](t, f)| \approx \dot{\varphi}(t), \quad (29)$$

and its amplitude A_r :

$$A_r(t) = \max_f |\mathbb{T}_\psi[u](t, f)| \approx A(t). \quad (30)$$

Other definitions of the ridge, or ridges of the CWT exist, in particular based on the study of its phase, but we will use this one for its simplicity and the stability of its numerical implementation [4].

3.2 Use for nonlinear, stationary systems under ambient excitation

By implementing the CWT on the response of a system described by Eq. (17) to an ambient excitation, we obtain from its ridge an estimate of the instantaneous frequency of the system (Eqs. (14) and (29)):

$$\Omega_{P,n} \approx 2\pi f_r(t_n), \quad (31)$$

and from its amplitude, an estimate of the amplitude of the system oscillations (Eq. (30)) :

$$|\underline{X}_n| \approx A_r(t_n). \quad (32)$$

Then, averaging f_r for a given A_r , we can estimate $\tilde{\omega}(A_0)$, the angular frequency of the undamped nonlinear system at amplitude A_0 (see Eq. (22)), and thus characterize its nonlinearity. Practically speaking, with numerical signals, it is very unlikely to obtain several times exactly the same value of A_r , and therefore impossible to average the values of f_r for a given A_r . To overcome this issue, it is possible to gather the values obtained for A_r into several small intervals, in order to obtain a sample large enough to average the corresponding f_r (similar to what can be done to compute a histogram for example).

Finally, obtaining an accurate ridge from the CWT (Eqs. (29) and (30)) is conditioned by the choice of a suitable quality factor Q . Several bounds exist in the literature, in particular for free responses [6, 7], ensuring among other things the separation of the different eigenfrequencies in the case of systems with several modes. It is therefore necessary to determine under which condition on the quality factor Q , the extraction of a ridge from the CWT gives accurate results for a system under ambient excitation. For this purpose, the time dispersion of the CWT, proportional to Q in the case of the Morlet wavelet, must be well below the characteristic time of variation of the signal amplitude, $A_{\text{ref}}/\dot{A}_{\text{ref}} \approx (\pi/\mu\omega_d)^{1/2}$. We then obtain, from Eqs. (10) and (12), the following bound:

$$Q \leq \frac{1}{c_A} \sqrt{\frac{\pi}{\zeta}}, \quad (33)$$

where c_A is a safety factor, reflecting the minimum ratio between the characteristic time of variation of the signal and that of the CWT. It will be set for the rest of this study at $c_A = 3$.

3.3 Use for nonlinear, nonstationary systems under ambient excitation

The method given in part 3.2 can also be used for nonlinear, nonstationary systems, provided that their non-stationarity can be explained by one or an array of known variables κ . Similarly to what is done for nonlinear, stationary systems, the range of (A, κ) has to be divided into small subsets, for which the corresponding instantaneous frequencies are averaged (see Eq. (24)). Obviously, the bound found for Q in Eq. (33) still has to be met, in order to get an accurate ridge.

A compromise has to be found between the number of subsets of (A, κ) and the number of associated observations of frequency $f_r(t_n)$. A too large number of subsets would cause a significant frequency scatter, due to the limited number of associated observations from which the averages are computed, while on the other hand a small number of subsets would result in a poor resolution in the (A, κ) space. In some cases, amplitude A or some of the explanatory variables of array κ contribute to a neglectible variation in frequency, and can therefore be ignored. The (A, κ) space can then be replaced by a smaller dimension space, drastically reducing the number of necessary subsets.

4 Numerical simulations

4.1 System under study

In order to illustrate the proposed method, numerical simulations of a nonlinear system under ambient excitation are carried out. The studied system is characterized by a piecewise linear rigidity function, presented

in Fig. 2, modeling an abrupt, asymmetrical softening.

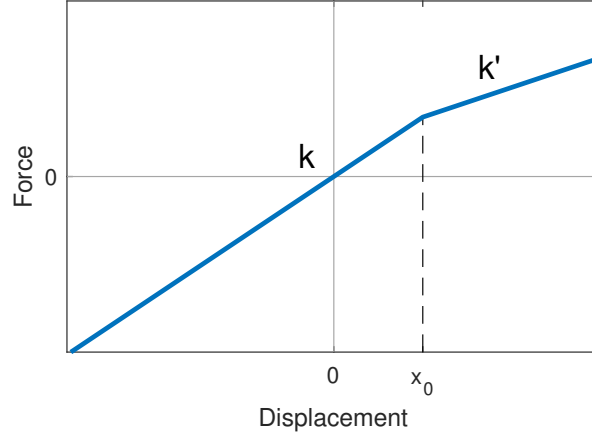


Figure 2: Rigidity function $x \mapsto kx + g(x)$ of the system under study.

Eq. (17), which governs the system dynamic behavior, is integrated numerically using the fourth order explicit Runge-Kutta method [15], with time step $\Delta t = 1$ ms. The system is assumed to be initially at rest, and a time interval for which it gains energy and reaches a nominal amplitude is discarded from the CWT analysis. This time interval is chosen five time larger than the system characteristic damping time, $(\zeta\omega_n)^{-1}$. The simulations total time is $T = 10000$ s. The modal parameters of the associated linear system (for $g = 0$), its natural frequency $f_n = \omega_n/2\pi$ and damping ratio ζ , are given in Table 1, along with informations on the nonlinearity function g and numerical integration.

Table 1: Numerical simulations parameters.

Numerical integration		Linear system		Nonlinearity	
T	Δt	f_n	ζ	x_0	k'
10000 s	1 ms	10 Hz	1 %	1	$k/2$

For the CWT computations, the Morlet wavelet is taken as mentioned before, with quality factor $Q = 5.91$, which corresponds to the upper bound introduced in Eq. (33). The CWT edge effect zones present at the beginning and end of the signal are discarded [6, 7].

4.2 First case study

For the first case study, excitation w is modeled as a white Gaussian noise, whose amplitude is chosen large enough so that x exceeds x_0 and triggers the nonlinear regime. This corresponds to the nonlinear, stationary system studied in part 2.2.

An extract of the response of the system obtained numerically is presented in Fig. 3, with its CWT. In Fig. 4, we can see the ridge extracted from this CWT as a function of its amplitude, along with its average at fixed amplitude, and the frequency of the undamped system (computed analytically using the principle of energy conservation).

We find a good agreement with the results expected in the analytical study. Indeed, Fig. 4a shows a dispersion of the system's instantaneous frequency inversely proportional to its amplitude, as stated in Eq. (16). Moreover, we can see in Fig. 4b that the average frequency of the system under ambient excitation seems to match its undamped frequency, as expected in Eq. (22), except for low and high amplitudes. The discrepancies at high amplitudes can easily be explained by statistical dispersion and can therefore be quantified, as such vibration amplitudes are scarce in the response sample. For low amplitudes however, there is a clear

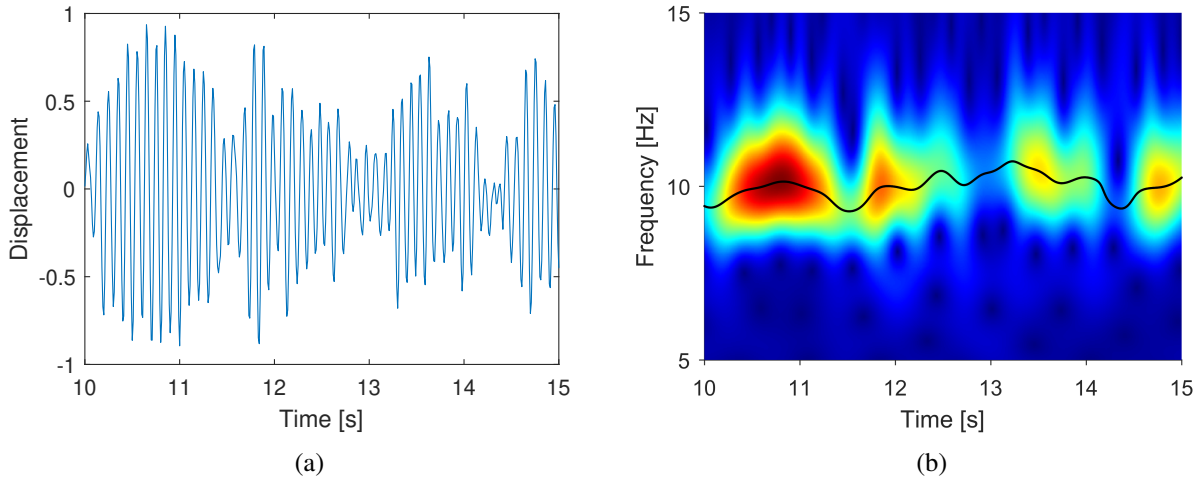


Figure 3: Numerical simulations, first case study: (a) extract of the system response x , (b) modulus of its CWT, with associated ridge (black curve).

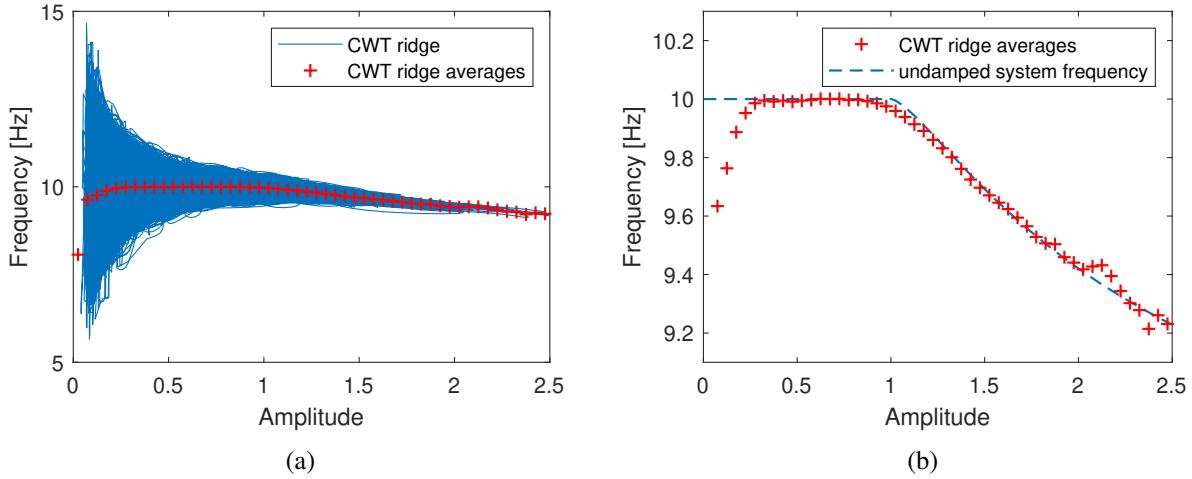


Figure 4: Numerical simulations, first case study: (a) CWT ridge f_r as a function of its amplitude A_r (blue), with its averages by amplitude increments of 0.05 (red), (b) CWT ridge averages (red), and undamped system frequency $\tilde{\omega}/2\pi$ (blue).

tendency to underestimate the frequency. This bias seems to be linked to the CWT analysis rather than to the approximations made in the modeling part, as a similar time-frequency signal processing tool, the Hilbert transform, was implemented as a substitute to the CWT and showed an inverse bias on the frequency (overestimating) for low amplitudes. Further numerical simulations showed a decreasing trend in this bias for lower values of system damping.

4.3 Second case study

For the second case study, excitation is modeled as a white Gaussian noise w , to which is added a “quasi-static” force F , harmonic with a period of 100 s. The amplitude of F is chosen high enough so that x_{stat} exceeds x_0 and triggers the nonlinear regime (see Eq. (25)), while that of w is chosen low enough so that $|x_{\text{dyn}}| \ll x_0$, and thus the amplitude of x_{dyn} provides a negligible contribution in the frequency variations of the system. This corresponds to the nonlinear, nonstationary equivalent system described in part 2.3, although it can be considered linear here because of the low dynamical vibrations amplitude.

In Fig. 5a, the ridge of the CWT of the system's response is presented as a function of its displacement x , along with its average at fixed displacement. This average is then compared in Fig. 5b to the undamped system frequency, which is computed analytically for a null vibration amplitude. The two curves show good agreement, except around x_0 where the CWT results do not exactly match the theoretical frequency discontinuity, but rather display a steep sigmoid. This is due to the influence of amplitude on the system's frequency, which does play a part around the slope change of the rigidity function at x_0 .

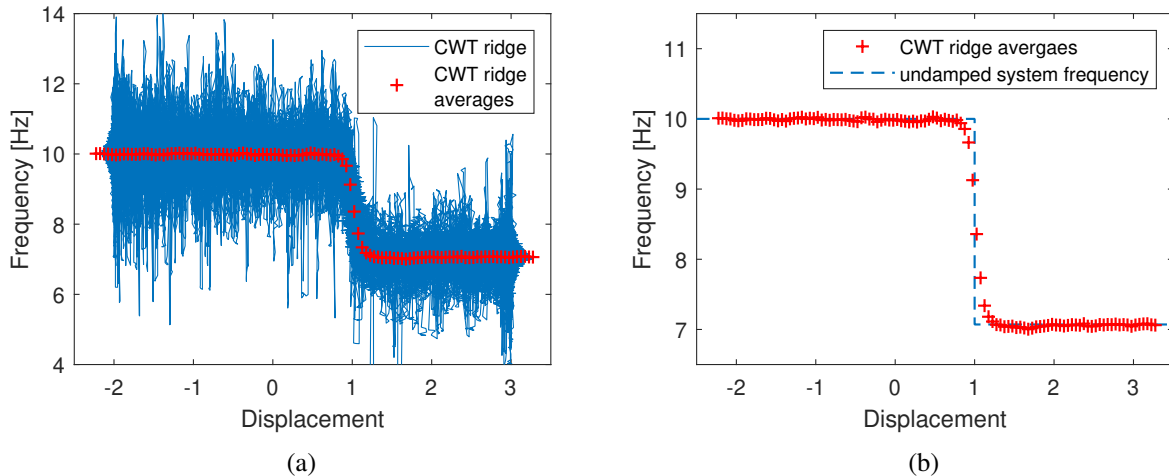


Figure 5: Numerical simulations, second case study: (a) CWT ridge f_r as a function of displacement x (blue), with its averages by displacement increments of 0.05 (red), (b) CWT ridge averages (red), and undamped system frequency $\tilde{\omega}/2\pi$ (blue).

5 Conclusions

The analytical study proposed in the first part, focusing on a weakly nonlinear and weakly damped mechanical system subjected to an ambient excitation, allowed to establish simple relationships regarding its instantaneous amplitude and frequency. In particular, it was shown that this frequency, at a given amplitude, is a random variable whose expectation is the system's free response frequency at that amplitude. These results were then generalized in the case of a nonstationary (nonlinear) system. The use of the CWT was then presented, to extract from the system's response its instantaneous amplitude and frequency. A new bound on the quality factor of the CWT, essential to obtain accurate results, was introduced. Finally, numerical simulations were performed on a simple case study. They showed good agreement between the theoretical and numerical results.

References

- [1] J.-J. Sinou, "A review of damage detection and health monitoring of mechanical systems from changes in the measurement of linear and non-linear vibrations," in *Mechanical vibrations: measurement, effects and control*, R. C. Sapri, Ed. New York: Nova Science Publishers, 2009, pp. 643–702, oCLC: ocn249134708.
- [2] S. Law and X. Zhu, "Dynamic behavior of damaged concrete bridge structures under moving vehicular loads," *Engineering Structures*, vol. 26, no. 9, pp. 1279–1293, Jul. 2004.
- [3] A. Graps, "An introduction to wavelets," *IEEE Computational Science and Engineering*, vol. 2, no. 2, pp. 50–61, 1995.

- [4] B. Torr sani, *Analyse continue par ondelettes*. EDP Sciences, Dec. 2012.
- [5] R. Carmona, W.-L. Hwang, and B. Torr sani, *Practical time-frequency analysis: Gabor and wavelet transforms with an implementation in S*, ser. Wavelet analysis and its applications. San Diego: Academic Press, 1998, no. v. 9.
- [6] T.-P. Le and P. Argoul, “Continuous wavelet transform for modal identification using free decay response,” *Journal of Sound and Vibration*, vol. 277, no. 1, pp. 73–100, Oct. 2004.
- [7] S. Erlicher and P. Argoul, “Modal identification of linear non-proportionally damped systems by wavelet transform,” *Mechanical Systems and Signal Processing*, vol. 21, no. 3, pp. 1386–1421, Apr. 2007.
- [8] N. M. Krylov and N. N. Bogoliubov, *Introduction to Non-linear Mechanics*. Princeton University Press, 1949.
- [9] W. J. Staszewski, “Identification of non-linear systems using multi-scale ridges and skeletons of the wavelet transform,” *Journal of Sound and Vibration*, vol. 214, no. 4, pp. 639–658, Jul. 1998.
- [10] J. Lardies and M.-N. Ta, “A wavelet-based approach for the identification of damping in non-linear oscillators,” *International Journal of Mechanical Sciences*, vol. 47, no. 8, pp. 1262–1281, Aug. 2005.
- [11] M. Brenner, “NON-STATIONARY DYNAMICS DATA ANALYSIS WITH WAVELET-SVD FILTERING,” *Mechanical Systems and Signal Processing*, vol. 17, no. 4, pp. 765–786, Jul. 2003.
- [12] T.-P. Le and P. Paultre, “Modal identification based on continuous wavelet transform and ambient excitation tests,” *Journal of Sound and Vibration*, vol. 331, no. 9, pp. 2023–2037, Apr. 2012.
- [13] T.-P. Le and P. Paultre, “Modal identification based on the time–frequency domain decomposition of unknown-input dynamic tests,” *International Journal of Mechanical Sciences*, vol. 71, pp. 41–50, Jun. 2013.
- [14] S. Nagarajaiah, B. Basu, and Y. Yang, “Output only modal identification and structural damage detection using timefrequency and wavelet techniques for assessing and monitoring civil infrastructures,” in *Sensor Technologies for Civil Infrastructures*. Elsevier, 2014, pp. 93–144.
- [15] J.-P. Demailly, *Analyse num rique et  quations diff rentielles*. Les Ulis: EDP sciences, 2006, oCLC: 494043512.